Strength and Fracture Toughness of the ESIS Silicon Nitride Reference Material

Tanja Lube[1], Robert Danzer[1], Jakob Kübler[2], Jan Dusza[3], Jean-Pierre Erauw[4], Hagen Klemm[5] and Vincenzo M. Sglavo[6]

[1] Institut für Struktur- und Funktionskeramik, Montanuniversität Leoben, A-8700 Leoben, Austria
[2] Swiss Federal Laboratories for Materials Testing and Research (EMPA), CH-8600 Dübendorf, Switzerland
[3] Institute for Materials Research, SAS Košice, SK-04353 Košice, Slovak Republic
[4] Belgian Ceramic Research Centre, B-7000 Mons, Belgium
[5] Fraunhofer Institut für keramische Technologien und Sinterwerkstoffe, D-01277 Dresden, Germany
[6] Dipartimento Ingegneria dei Materiali, Università di Trento, I-38505 Trento, Italia

ABSTRACT: *The ESIS Technical Committee for Ceramics (TC6) is running a joint program to characterise a commercial silicon nitride ceramic with respect to all properties necessary to a proper design process. In this paper some preliminary results of measurements on the ESIS Reference Silicon Nitride are presented: the room temperature 4-pt. bending strength is around 870 MPa and the 3-pt. bending strength is around 990 MPa. These two data clearly demonstrate the volume dependence of strength, which can consistently be described with the Weibull theory and a Weibull modulus of about 15. The room temperature fracture toughness of the material is 4,9 MPam$^{1/2}$ (determined with the SEVNB method). IF-toughness values are between 4,8 to 7,9 MPam$^{1/2}$. Although some sub-critical crack growth exists at room temperature (the crack growth exponent is around 50), severe time dependent damage starts around 1000°C.*

INTRODUCTION

In a joint European research program organised by the European Structural Integrity Society (ESIS) a complete set of material properties indispensable for design (including crack extension parameters, cyclic fatigue data and data correlated to contact mechanical problems) will be measured for a commercial silicon nitride grade. A more detailed description of this program can be found in [1].

Investigated Material

The investigated material is the SL200-B gas pressure sintered silicon nitride doped with Al_2O_3 and Y_2O_3 made by CeramTec, Plochingen, Germany. Details on the microstructure can be found in [2].

Strength Testing

Specimens with dimensions according to EN843-1 [3] for all strength test were diamond machined from larger plates [2] and finished with a D15-diamond grit disc on the tensile surface. Bend tests were performed on fully articulated jigs. Strength tests at elevated temperatures were performed after heating the specimens at 25 – 30 °C/min and a subsequent dwell time of 5 min. The statistical evaluation was made according to ENV843-5 [4].

Fracture Toughness Testing

Fracture toughness was tested using the SEVNB-method [5, 6], the SEPB-method [7] and the IF-method [8, 9]. The pre-cracks for the SEPB method were introduced by the method proposed in [10]. To measure the influence of the crack length on the toughness (i.e. the R-curve), stable crack growth experiments using the method described in [10] were used.

Sub-critical crack growth testing

Static 4-point bend tests on standard bend bars in ambient air were used to investigate the influence of time on strength at temperatures up to 1200°C. At room temperature tests were conducted in deionized water. At least three different stress levels per temperature were investigated, the tests were suspended after 168 h if a specimen did not fail. From the experimental raw data crack growth data for *v*-*K*-curves were evaluated using the 'modified' evaluation proposed in [11].

STRENGTH AND TOUGHNESS AT ROOM TEMPERATURE

Strength

The results of 4-point and 3-point bending strength tests results are shown in a Weibull-plot in Fig. 1. The relative probability of failure is plotted against the strength in such a way that the Weibull distribution is represented as a straight line [11-14].

In the case of the 4-point bending tests 55 experiments performed by two laboratories (27 (lab A) and 28 (lab B) tests in each set) are shown. The characteristic strength of set A is $\sigma_{0,A} = 853$ MPa and that of set B is $\sigma_{0,B} = 882$ MPa. With respect to the inherent scatter of the data both strength values have to be considered equal within a 95 % confidence limit and the

common characteristic strength value is 869 ± 15 MPa[1]. The individual data points of both tested sets are nicely arranged on a straight lines indicating that the strength values are two-parameter Weibull distributed. The slope of this line indicates the Weibull modulus: $m_{4PB} = 14 \pm 2$[1].

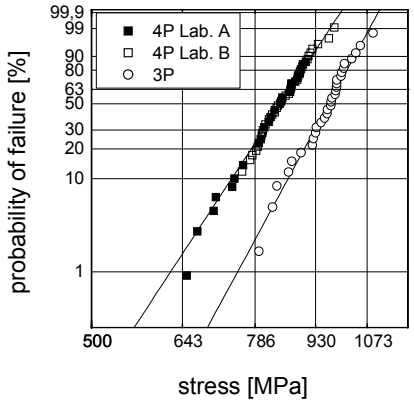

Fig. 1: Weibulldiagram of 3 point bend tests and 4-point bend tests.

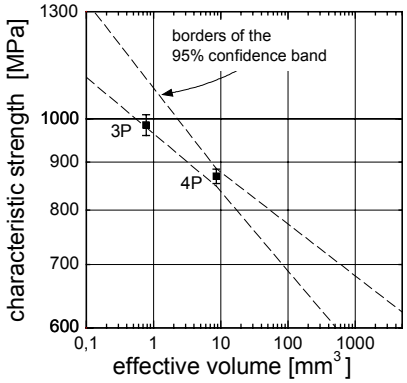

Fig. 2: Dependence of the characteristic strength on the effective volume.

The single set (30 tests – lab C) of 3-point bending strength results also obeys the Weibull distribution. Obviously the characteristic strength is much higher ($\sigma_{0,C} = 985 \pm 25$ MPa[1]) but the Weibull modulus is almost equal ($m_{3PB} = 16 \pm 5$[1]). The increase in the characteristic strength is a consequence of the "size effect", which is the most important consequence of the Weibull theory [11-16]. The strength decreases, if the volume under load (effective volume) increases. This is shown in Fig. 2, where the characteristic strength is plotted versus the effective volume. Again the Weibull behaviour is indicated by a straight line. From its reciprocal slope the Weibull modulus for all two types of tests can be determined, yielding $m = 18$. In Fig. 2 the 95 % confidence limits for the data evaluation due to the inherent scatter are indicated by dashed lines. It can clearly be recognised, that all data fit well together.

This kind of data evaluation is only meaningful, if the fracture origins are all volume or all surface defects. Therefore a fractographic analysis of the data is necessary [16]. This analysis is just at the beginning but some first results (Fig. 3) demonstrate, that the fracture origins are material inherent defects that correspond to the defects found on polished sections [1].

[1] The numbers after the '±' character indicate the limits of the 95% confidence interval according to [4] and not a standard deviation as in all other cases of this paper.

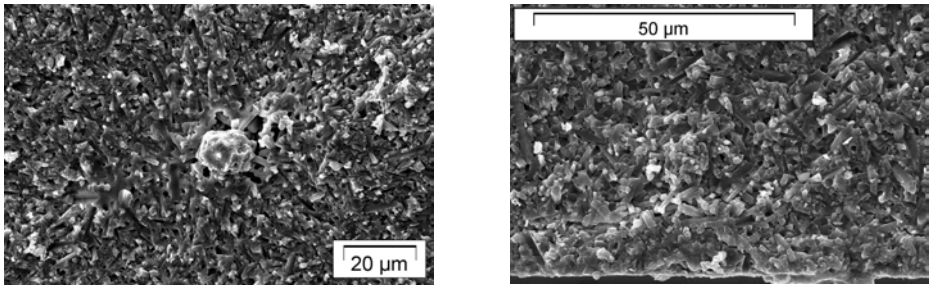

Fig. 3: Fracture origins in bend specimens: a) volume defect: Iron-inclusion, b) defect close to surface: insufficiently compacted region.

Thoughness

An overview of values for the fracture toughness determined using different methods is given in Table I.

Table I: Fracture toughness results.

method	K_{Ic} **[MPa m$^{1/2}$]**
SEVNB [5, 6]	4,94 ± 0,06
SEPB [7]	4,67 ± 0,19
IF [8] (median cracks)	7,9 ± 1,19
IF [9]	4,8 ± 0,6

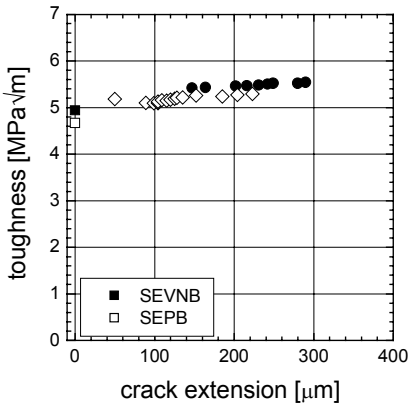

Fig. 4: $K_{Ic,0}$ values measured with the SEVNB and the SEPB technique and R-Curve.

The SEVNB and SEPB results correspond nicely. The higher value obtained with the SEVNB method may be attributed to the shielding effect of the notch [17] which may cause an overestimation of the fracture toughness.

The values calculated with the two different formulas for the indentation fracture method impressively show the typical large variability in results that may be obtained with this method. The formula after [8] was calibrated using different brittle materials while the equation proposed by [9] was adjusted to different Si_3N_4-alloys.

The data shown in Fig. 4 indicate only a moderate increase of fracture toughness as the crack grows. This result is consistent with the microstructure and other observations on the R-curve behaviour of silicon nitrides [18]: the grains are only moderately elongated and may only act as effective bridging elements over a very short distance during crack growth.

STRENGTH AT ELEVATED TEMPERATURES

Some first test results at elevated temperatures are shown in Fig. 5. The data at 800°C and at 1000°C show a slight decrease of strength. At even higher temperatures the decrease of strength is more pronounced.

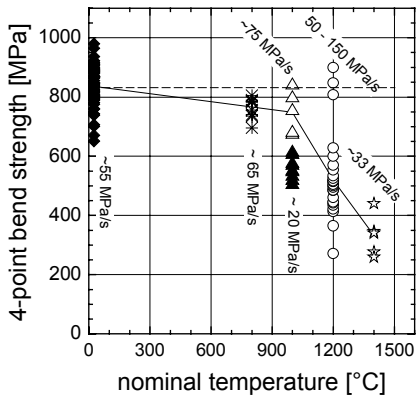

Fig. 5: Temperature dependence of 4-point bend strength. The mean loading rate for the test series is indicated in the diagram. Tests were performed by five different labs.

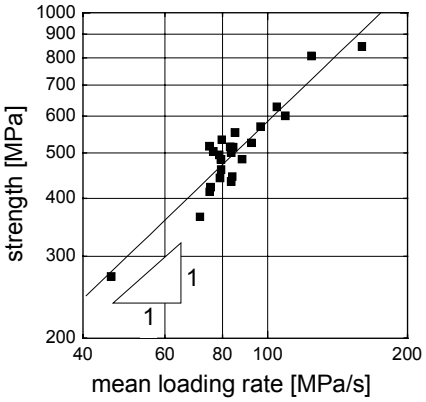

Fig. 6: Influence of loading rate on fracture strength at 1200°C, constant load rate tests are not shown in this diagram.

It is well known, that in this temperature region subcritical crack growth or creep gain influence and can cause a drop of strength [14]. The strength can strongly depend on the rate and mode of loading[2] [19]. Strength data determined at 1200°C are plotted versus the "mean" loading rate (calculated as strength divided by test duration) in Fig. 6. A linear increase of strength with loading rate can be observed. In general such a behaviour can be explained by the fact, that at a high loading rate, subcritical crack growth or creep can occur to a lesser extent than at a low strain rate. Consequently, the strength is higher at high loading rates [19]. The linear dependence of strength on loading rate in Fig. 6 is a hint, that diffusional creep [19] is the relevant damage mechanism at 1200°C. A fractographic analysis, which could help to confirm this assumption has not yet been completed.

It follows from the behaviour shown in Fig. 5, that at sufficient high loading rates, the room temperature strength can be maintained up to 1000°C or even to higher temperatures (as indicated by the dashed line). At

[2] Of course, a stress rate sensitivity of the strength also exists at room temperature, as will be shown in the next chapter, but it is much less pronounced than at high temperatures.

temperatures above 1000°C, the strength of the material is severely dependent on the loading rate.

THE INFLUENCE OF TIME ON STRENGTH

The influence of time under load on the strength was investigated by static bend tests. The measured lifetimes varied by up to six orders of magnitude for a single load level at a given temperature. Results for tests at room temperature/100% relative humidity and 1000°C/ambient air are show in Fig. 7.

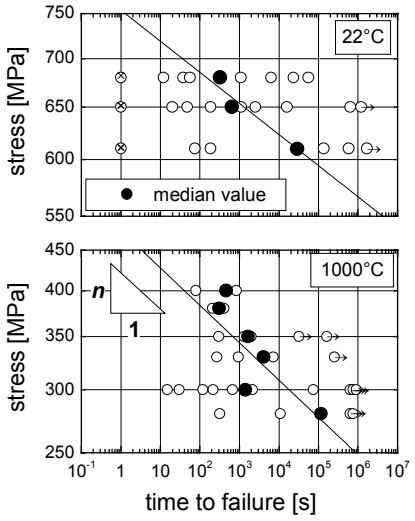

Fig. 7: Lifetime of the ESIS silicon nitride in deionized water at 22°C and in ambient air at 1000°C. × denotes spontaneous failure, → denotes suspended tests.

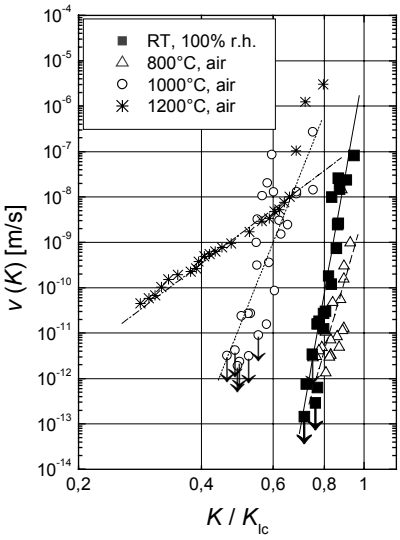

Fig. 8: *v*-*K*-curves for four different temperatures. Arrows indicate suspended tests. The crack geometry factor was assumed to be $Y = 1{,}3$.

The observed behaviour can be explained by sub-critical crack growth (i.e. at stress intensities below the fracture toughness) [14] of existing defects. The large scatter in lifetimes is caused by the size distribution of the initial defects. The same size distribution is also the reason for the scatter of the strength.

The sub-critical crack growth behaviour is usually described by an empirical power law relation between the crack growth rate v and the applied stress intensity K:

$$v = A^* \cdot \left(K / K_{\mathrm{Ic}}\right)^n \quad . \tag{1}$$

The material and temperature dependent parameters A^* and n can be determined from the plot shown in Fig. 7 [11] (open symbols in Fig. 9).
If information on the strength under inert conditions and the geometry of the defects is available, the crack growth rate can be determined directly from the experimental data [11] without having to assume a special relation between crack velocity and applied stress intensity. The arrangement of the data points on a straight line in Fig. 8 indicates, that the power law (1) is indeed a suitable description of the observed crack growth behaviour. It is notable that it was possible to investigate cracks that grow as slow as 10^{-13} m/s with this method.

The high temperature tests may be evaluated according to the same procedure. For the evaluation shown in Fig. 8 the fracture toughness was taken to be independent of temperature. This is a questionable assumption because an increase of toughness is expected to occur near the glass transition temperature (~ 950°C [20]). This would shift the data along the *x*-axis to the left hand side of the diagram, but would not affect their slope. As indicated in the previous section it is also not clear, if the dominant failure mechanism at high temperatures is sub-critical growth of a single defect or if delocalised damage (i.e. creep) occurs.

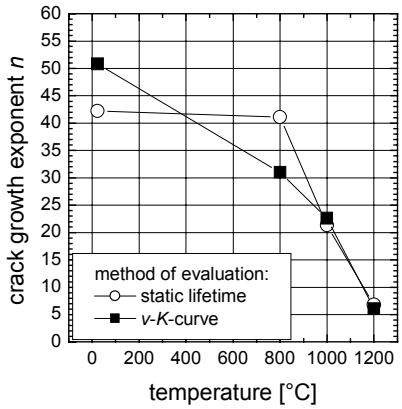

Fig. 9: Comparison of values for the crack growth exponent *n*: comparison of two different evaluation methods and temperature dependence.

A comparison of the values for the crack growth exponent *n* determined with the two presented methods and its dependence on temperature can be seen in Fig. 9.

SUMMARY AND OUTLOOK

The first results of investigation on the strength properties of the ESIS silicon nitride were presented. The material may now be classified in the range of commercial available silicon nitrides. The results in hand indicate that the materials has only a limited high temperature potential due to

pronounced damage by creep or sub-critical crack growth.

The identification of failure initiating defects and the clarification of the dominant failure mechanisms is still in progress. It can be expected that a data collection usable for design purposes will be available within the next two years.

REFERENCES

1. Lube, T., Danzer, R., Steen, M. (to be published) *Improved Ceramics Trough New Measurements, Processing and Standards*, Proceedings of PacRim 4, Nov. 4.8, 2001, Wailea, Hawaii, USA
2. Lube, T., Danzer, R. (to be published), Proc. of ECF 14, Cracow, Sept. 8-13, 2002
3. EN 843-1, Advanced Technical Ceramics - Monolithic Ceramics - Mechanical Properties at Room Temperature: Part 1 - Determination of Flexural Strength. 1995
4. ENV 843-5, Advanced Technical Ceramics - Monolithic Ceramics - Mechanical Properties at Room Temperature: Part 5- Statistical Evaluation. 1997
5. Kübler, J. (2000) *Procedure for Determining the Fracture Toughness of Ceramics Using the Single-Edge-V-Notched Beam (SEVNB) Method*. GKSS-Forschungszentrum on behalf of the European Structural Integrity Society, Geesthacht.
6. Kübler, J. (2002). In: *Fracture Resistance Testing of Monolithic and Composite Brittle Materials, ASTM STP 1409*, p. 93, Salem, J.A., et al. (Ed.). American Society for Testing and Materials, West Conshohocken.
7. ASTM C 1421-99, Standard Test Methods for Determination of Fracture Toughness of Advanced Ceramics at Ambient Temperature. 1999
8. Niihara, K., Morena, R., Hasselman, D.P.H. (1982) *J. Mat. Sci. Let.*, **1**, 13.
9. Lewis, M.H., Fung, R., Taplin, D.M.R. (1981) *J. Mat. Sci.*, **16**, 3437.
10. Pancheri, P., Bosetti, P., Dal Maschio, R., Sglavo, V.M. (1998) *Eng. Fract. Mech.*, **59**, 4, 447.
11. Munz, D., Fett, T. (1999) *Ceramics*. Springer, Berlin, Heidelberg.
12. Weibull, W. (1939) *A Statistical Theory of Strength of Materials*. Royal Swedish Institute for Engineering Research, Stockholm.
13. Weibull, W. (1951) *Journal of Applied Mechanics*, **18**, 293.
14. Wachtman, J.B. (1996) *Mechanical Properties of Ceramics*. Wiley-Interscience, New York, Chichester.
15. Danzer, R. (1992) *J. Eur. Ceram. Soc.*, **10**, 461.
16. Danzer, R., Lube, T., Supancic, P. (2001) *Zeitschrift für Metallkunde*, **92**, 7, 773.
17. Kübler, J., Danzer, R., Fett, T., Damani, R. (1999). In: *Fracture Toughness of Ceramics Using SEVNB Method Round Robin*, Kübler, J. (Ed.). VAMAS Report No. 37, ESIS Document D2-99
18. Becher, P.F., et al. (1998) *Journal of the American Ceramic Society*, **81**, 11, 2811.
19. Danzer, R. (1988) *Lebensdauerprognose hochfester metallischer Werkstoffe im Bereich hoher Temperaturen*. Gebrüder Borntraeger, Berlin, Stuttgart.
20. Roebben, G., Erauw, J.P., Lube, T., Duan, R.G., Cambier, F., Van der Biest, O. (to be published), Proc. of ECF 14, Cracow, Sept. 8-13, 2002